HHS Public Access

Author manuscript

J Phys Chem B. Author manuscript; available in PMC 2019 July 19.

Published in final edited form as:

J Phys Chem B. 2018 July 19; 122(28): 7049–7056. doi:10.1021/acs.jpcb.8b04647.

Dependence of the Formation of Tau and Aβ Peptide Mixed Aggregates on the Secondary Structure of the N-terminal Region of Aβ

Ana V. Rojas[†,*], **Gia G. Maisuradze**[‡,*], and **Harold A. Scheraga**[‡,*]

[†]Schrödinger, Inc., 120 West 45th Street, New York, NY 10036

[‡]Baker Laboratory of Chemistry and Chemical Biology, Cornell University, Ithaca, NY 14853

Abstract

One of the hallmarks of Alzheimer's disease is the formation of aggregates of the tau protein, a process that can be facilitated by the presence of fibrils formed by the Amyloid β peptide (Aβ). However, the mechanism that triggers tau aggregation is still a matter of debate. The effect of $A\beta_{40}$ fibrils on the aggregation of the repeat domain of tau (TauRD) is investigated here by employing coarse-grained molecular dynamics simulations. The results indicate that the repeat domain of tau has high affinity for $A\beta_{40}$ fibrils, with the $_{261}$GSTENLK$_{267}$ fragment of tau driving TauRD towards the $_{16}$KLVFFA$_{21}$ fragment in $A\beta_{40}$. Monomeric $A\beta_{40}$, in which the $_{16}$KLVFFA$_{21}$ fragment is rarely found in an extended conformation (as in the fibril), has low affinity for the TauRD, indicating that the ability of $A\beta_{40}$ fibrils to bind to the TauRD depends on the $_{16}$KLVFFA$_{21}$ fragment of Aβ adopting an extended conformation.

Graphical Abstract

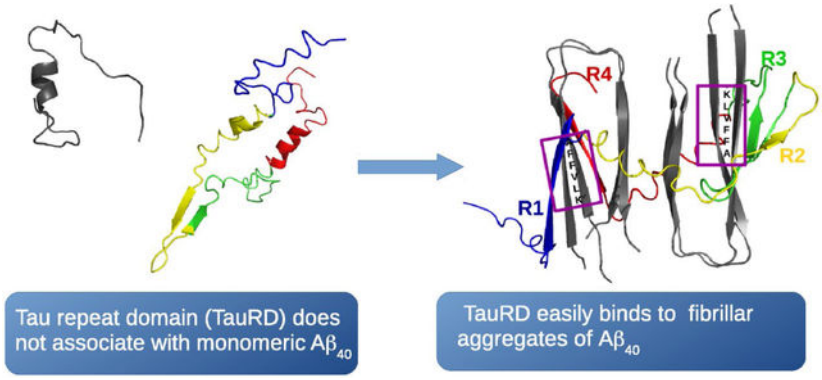

*To whom correspondence may be addressed. avr5@cornell.edu; gm56@cornell.edu; has5@cornell.edu.

Author Contributions: A.V.R. designed the research; A.V.R. and G.G.M. performed the research; A.V.R. and G.G.M. analyzed the data; and A.V.R., G.G.M., and H.A.S. wrote the paper.

Supporting Information

The Supporting Information is available free of charge on the http://pubs.acs.org

Formation of β-hairpin in Tau3RD and Tau4RD; Histograms of radius of gyration for Tau4RD and Tau3RD in the presence and absence of the $A\beta_{40}$ template; TauRD's binding affinity to non-aggregated $A\beta_{42}$ monomers.

The authors declare no competing financial interest.

Introduction

The brain of patients with Alzheimer's disease (AD)[1] presents extracellular plaques formed by fibrils of the Amyloid β peptide (Aβ) and intracellular tangles of a different fibrillar material, often referred to as paired helical filaments (PHFs), formed by the tau protein[2]. A number of studies have indicated that these two events are deeply connected[3-6]. Unlike Aβ, which aggregates easily and forms fibrils both *in vitro* and *in vivo*, tau is highly soluble and does not aggregate normally[7-8]. The widely accepted "amyloid hypothesis"[9] states that Aβ fibrils appear early in the disease, and they facilitate the aggregation of tau. According to this hypothesis, it is through the tau aggregates that Aβ exerts its toxicity, causing neuronal degeneration and death[9-10].

Many studies have shown that Aβ fibrils and pre-fibrillar amyloids can facilitate tau aggregation[3-4, 11-13]. Aβ and tau can form mixed aggregates[11-12], and this interaction might promote aggregation-prone conformations in tau. Aβ can also precipitate the formation of the PHFs of tau by a more complex mechanism, in which Aβ facilitates hyperphosphorylation of tau, which in its turn can lead to fibrillization of tau[3, 11, 14]. Hence, it is clear that interaction with Aβ can trigger aggregation of tau. However, the details of this interaction – critical for the design of drugs aimed to prevent it – are not well understood.

In addition, it is not clear which species of Aβ (soluble, fibrillar or pre-fibrillar) or which isoform ($A\beta_{40}$ or $A\beta_{42}$) is responsible for Aβ-induced aggregation of tau. While some studies have indicated that in soluble form, only $A\beta_{42}$, and not $A\beta_{40}$, can trigger tau hyperphosphorylation and aggregation[14], others have shown that in their fibrillar form both $A\beta_{40}$ or $A\beta_{42}$ can produce the same effect[3, 11]. Intriguingly, another study has shown that pre-fibrillar aggregates of $A\beta_{42}$, but not monomers or fibrils, can facilitate the formation of tau trimers that can subsequently associate into PHF[13]. The contradictory results regarding the Aβ species implicated in tau aggregation might arise from the fact that $A\beta_{42}$ aggregates at a much faster rate than $A\beta_{40}$[15]. Therefore, experiments using soluble $A\beta_{42}$ might have $A\beta_{42}$ aggregates within minutes of mixing, while samples containing $A\beta_{40}$ will take longer to develop aggregates and will contain mostly monomeric $A\beta_{40}$. Another source of contradiction is the fact that Aβ fibrils, or smaller aggregates, prepared by different protocols can have different morphologies[16]. Hence, two different samples of $A\beta_{42}$ fibrils, each with a particular morphology, might interact very differently with tau and produce a very different result. Therefore, it is important to understand the structural principles governing the interaction between Aβ and tau. With this goal in mind, in this article, the effect of $A\beta_{40}$ fibrils and monomers on the aggregation of the repeat domain of tau is investigated using molecular dynamics (MD) simulations with the coarse-grained united-residue (UNRES) force field[17-21].

Methods

The UNRES model.

Detailed descriptions of the UNRES model and its parametrization are available in references [17-20, 22-23]. The implementation used here to simulate multichain complexes was reported in reference [22]. Here, for completeness, we give a short description of the model. In

the UNRES model,[17-20, 22-23] a polypeptide chain is represented as a sequence of α-carbon (C^{α}) atoms with united peptide groups (p) located halfway between the consecutive C^{α} atoms and united side chains (SC) attached to the C^{α} atoms. The force field has been derived as the potential of mean force (PMF) of a system of polypeptide chain(s) in water, where all degrees of freedom except the coordinates of the C^{α} atoms and SC centers have been averaged out[17, 20]. The effective energy function contains local and site-site interactions, as well as multibody terms, which have been obtained by decomposing the PMF into factors corresponding to clusters of interactions within and between coarse-grained sites[17]. The SC-SC interaction potentials implicitly include the contribution from solvation[17, 20]. The force field was calibrated to reproduce the structure and thermodynamics of small model proteins[18-19, 23]. In this study, the parameters derived from the study of the WW domain from the Formin-binding protein 28 (PDB ID: 1E0L)[19] were used.

Simulation setup.

In simulations that included an $A\beta_{40}$ template, the template was modeled using the coordinates derived by Petkova et al.[24] (Fig. 1). Our previous study on this system[25] showed that a large fibril can be mimicked by using only two layers. Therefore, the template used in this work consisted of two layers, resulting in a total of 4 chains. To give the template the stability of a long fibril, distance restraints were applied to the C^{α} carbons as in reference 45. The free monomer was initially placed at a 20 Å distance from the edge of the template in a random coil conformation (Fig. 1). When simulations included two free monomers, the second monomer was placed 20 Å away from the first, and 20 Å from the template. In simulations that included only free monomers, the chains were initially in an extended conformation, parallel to each other, and separated by 20 Å distance. In all simulations the system was enclosed in a spherical volume, as in reference [25], the size of which was set to result in a concentration of 3 mM.

Molecular dynamics (MD) simulations.

Simulations were carried out using replica exchange molecular dynamics (REMD). For each system, a total of 120 trajectories were simulated with temperatures ranging from 280 K to 320 K. Each trajectory was 72×10^5 steps long, which was equivalent to 3.6×10^5 UNRES molecular time units (mtu),[26] which is approximately 17.6 μs. Based on previous benchmarks[26], a time step of 0.05 mtu was used, with a variable-time-step algorithm[27]. Temperature exchanges were attempted every 20,000 steps. Between exchanges, the temperature was held constant with the Berendsen thermostat[28].

When averages such as β-content, radius of gyration or number of hydrogen bonds are reported, they are obtained by averaging over conformations from the last 22×10^5 steps and using only conformations from simulations at 300 K. When the number of trajectories showing dimers is reported, the values are obtained using all conformations.

To calculate the fraction of trajectories that resulted in binding of the tau fragment (either one or several repeats) to the template, we used 3 amino acids long β-sheet as the cutoff. In other words, if the monomer formed a β-sheet with the template that was at least 3-amino acids long, then it was considered to be bound to the template.

The binding propensity of Tau3RD and Tau4RD along the $A\beta_{40}$ sequence, which are shown in Figure 2a, have been averaged over all the chains (i.e, divided by 4). This was done because for some trajectories, the tau fragment binds across the surface of the template, and often to the same region of $A\beta_{40}$ (as in Fig. 2b), resulting in double counting of the binding at that region. Therefore, to obtain a measure of binding propensity that was independent of the number of exposed chains, the results were averaged over all the chains in the template.

Results and Discussion

Six different tau isoforms exist[29-30] in the human brain. The longest tau isoform, htau40, is 441 residues long (Fig. 3a). The C-terminal half of tau contains what is known as the repeat domain (Fig. 3b). Three of the six tau isoforms contain four repeats (R1 to R4), but the other three contain only three of the repeats (R1, R3 and R4). Both three- and four-repeat isoforms are found in tau filaments from AD brains[31]. The repeat domain of tau (TauRD) forms the core of tau fibrils[32] and promotes β-sheet formation[33-36]. Therefore, we focused our study on this region, more specifically on the three-repeat (Tau3RD) and the four-repeat (Tau4RD) tau fragments (Fig. 3c). For this purpose, we carried out MD simulations of a 4-chains (2 layers) $A\beta_{40}$ template[24] interacting with Tau3RD or Tau4RD (Fig. 1).

Results show that Tau3RD and Tau4RD have high affinity for the $A\beta_{40}$ template.

The tau monomer forms hydrogen bonds with the template in 69% of Tau4RD trajectories and in 67% of Tau3RD ones. By tracking the regions of $A\beta_{40}$ participated in the hydrogen bonds formed with Tau3RD or Tau4RD, and averaging over the four chains in the template, a binding propensity along the $A\beta_{40}$ sequence was calculated (Fig. 2a). The results show that the residues in $A\beta_{40}$ responsible for the binding to Tau3RD and Tau4RD are primarily residues along the N-terminal half of $A\beta_{40}$ (see Fig. 2a and 2b), with the highest binding propensity seen along the KLVFFA fragment (residues 16-21) of $A\beta_{40}$.

In order to describe, in detail, the pathway along which the tau monomer binds to the fibril template, we built the free-energy landscape (FEL) along the principal components (PCs) (Fig. 4) obtained from principal component analysis (PCA) of a representative trajectory. PCs typically capture most of the total displacement from the average protein structure with the first few PCs during a simulation[37-39]. It appears that, at an early stage in the trajectory, the GSTENLK fragment of Tau4RD (residues 18-24 of the R1 repeat) drives the tau protein towards the KLVFFA fragment (residues 16-21) of one of the $A\beta_{40}$ chains, and binds this fragment forming a β-sheet (representative structures of minima 2-6). The R2, R3 and R4 repeats do not interact with the $A\beta_{40}$ template during this time interval. Only after finishing formation of the β-strand and binding of the R1 repeat with the $A\beta_{40}$ template, does the R4 repeat start moving towards the second semifilament of the $A\beta_{40}$ template, and the GSLDNIT fragment (residues 19-25 of R4 repeat) binds to the KLVFFA fragment of one of the chains with anti-parallel orientation and forms a β-strand (see representative structures of minima 7-9 in Fig. 4 and Fig. 2b). The highest affinity is seen along a region of $A\beta_{40}$ containing the KLVFFA sequence (Fig. 2a). Interestingly, the KLVFFA fragment has been shown to be critical for the formation of Aβ fibrils[40-41]; it is also capable of forming

amyloid fibrils by itself and to sequester small compounds into these fibrils[42]. Our simulations show that this same region is critical for interaction with Tau3RD and Tau4RD.

It is interesting to note that Tau4RD and Tau3RD show a considerable amount of α-helical structure throughout the simulations (see representative structures of minima in Fig. 4). These helices are quite flexible and often unfold or convert into β-sheets. However, it is evident that the presence of the $A\beta_{40}$ template can offset the β-sheet-to-α-helix balance in the tau fragments by stabilizing β-sheets with the template.

Tau3RD and Tau4RD exhibit higher β-sheet content in the presence of the $A\beta_{40}$ template.

To further understand the effect of the $A\beta_{40}$ template on the secondary structure of the tau fragments, simulations of Tau3RD or Tau4RD, without the $A\beta_{40}$ template, were carried out, and compared with those with the $A\beta_{40}$ template. These comparisons show that the $A\beta_{40}$ template promotes conformations with higher β content along Tau3RD and Tau4RD (Fig. 5). The increase in β content is primarily due to β-sheets between $A\beta_{40}$ and the R1 or R4 repeats of tau. This can be seen when evaluating the probability of each residue on the tau repeat to form a hydrogen bond with the $A\beta_{40}$ template (Fig. 6, top and middle panels). Areas with higher probabilities (i.e., areas that often form hydrogen bonds with the $A\beta_{40}$ template) are those that are frequently involved in β sheets with the $A\beta_{40}$ template. Therefore, our simulations indicate that binding occurs more often through hydrogen bonds involving residues along repeats R1 and R4 (Fig. 6, top and middle panels).

Interactions between tau repeats hinder their ability to bind to the $A\beta_{40}$ template.

The lower tendency of repeats R2 and R3 to form hydrogen bonds with the Aβ peptides could be due to their sequence having low affinity with Aβ or to interactions between the repeats (R2 and R3 with each other or with the other repeats) competing with the tau-Aβ interactions. To investigate this question, simulations of each of the repeats (R1, R2, R3 or R4) interacting with an Aβ template were carried out. The tendency of each of the repeats to form hydrogen bonds with the template is shown in Fig. 6, bottom panel. These results indicate that, when the other repeats are absent, each of the four repeats has similar affinity with the peptides in the $A\beta_{40}$ template. Moreover, their tendency to form hydrogen bonds with the template is higher when they interact with the template by themselves than when the other repeats are also present (Fig. 6). Therefore, interactions between the repeats must be hindering binding to Aβ. Indeed, the fragment $_{306}$VQIVYK$_{311}$, the regions with the highest β-structure potential in tau[33], is often seen forming a β-hairpin in our simulations (Fig. S1a-c). This β-hairpin is present in simulations of monomers, as well as in simulations with the template, and it forms in early stage of the simulations (Fig. S2 and S3), indicating that its formation and stabilization is due to intramolecular contacts and does not depend on interactions with the $A\beta_{40}$ template. This suggests that the presence of the β-hairpin might hamper the ability of the regions involved in it to bind to the $A\beta_{40}$ template.

The presence of the $A\beta_{40}$ template does not facilitate dimerization of TauRD.

The fact that, upon interacting with the Aβ template, Tau3RD and Tau4RD show an increase in their β-sheet content suggest that the presence of Aβ might make tau more prone to aggregation. To investigate this, MD simulations of dimers of Tau3RD or Tau4RD with or

without an Aβ template were carried out. The MD simulations were partitioned into twelve consecutive intervals, and the average number of trajectories in which a β-sheet had formed between the TauRD monomers were calculated. The results show different behaviors for Tau3RD and Tau4RD. Consistent with aggregation experiments[8], Tau4RD shows a higher tendency to form homodimers than Tau3RD (Fig. 7). Contrary to our expectations, the presence of the template does not seem to affect the formation of dimers by Tau3RD or Tau4RD (Fig. 7).

Although our simulations do not show a higher rate of dimerization in the presence of the Aβ template, it is possible that this is an effect that cannot be observed within the time scale of our simulations, or that it cannot be seen on the Tau3RD or Tau4RD fragments, but that the complete tau protein needs to be simulated. Another possibility is that a larger number of monomers need to attach to the Aβ template for aggregation to be observed. It should also be mentioned that the only experimental evidence of Aβ alone been capable of triggering tau aggregation is a study where tau peptides were subjected to several rounds of incubation with decreasing levels of Aβ aggregates before the presence of tau trimers (not PHFs) was detected[13]. Therefore, it is possible that the increase in β-sheet content on tau observed in our simulations (Fig. 5) might result, after hours of incubation and several remixing steps, in tau oligomerization. Aβ-induced aggregation of tau was also studied through MD simulations by Qi et al.[43]. Their simulations indicated that an $A\beta_{42}$ template causes Tau3RD and Tau4RD fragments to adopt more extended conformations, which would presumably facilitate their assembly into fibrils. This “stretching-and-packing”[43] mechanism was reflected in their simulations in higher radii of gyration when the fragments interacted with the $A\beta_{42}$ template, i.e., the presence of the template caused the tau fragments to stretch out. Our simulations did not show this effect. While the radii of gyration that we obtain (Fig. S4) are more consistent with a disordered peptide[44], we do not see any significant difference between the simulations of a free monomer and those of a monomer and a template. The discrepancies between our results and those of Qi et al.[43] might be attributed to differences in the force fields or effective simulation times, but they can also arise from the fact that our simulations were carried out with an $A\beta_{40}$ template instead of $A\beta_{42}$.

TauRD’s binding affinity to $A\beta_{40}$ is largely reduced when $A\beta_{40}$ is a non-aggregated form.

Many experimental studies have indicated that $A\beta_{42}$, but not $A\beta_{40}$, can induce tau aggregation[14, 45]. However, these studies often use the Aβ peptides in a non-aggregated state[14]. Because $A\beta_{42}$ aggregates at a faster rate than $A\beta_{40}$, the studies might be evaluating the effect of different aggregation states. This possibility was pointed out in a study by Rank et al[11], where the authors found that soluble $A\beta_{42}$, but not $A\beta_{40}$, could form mixed aggregates with tau. However, if pre-aggregated $A\beta_{40}$ was used, the effect on tau aggregation was similar to that of non-aggregated $A\beta_{42}$.

To see if, as in Rank et al.[11] experiments, the ability of $A\beta_{40}$ to bind to Tau3RD and Tau4RD fragments was only seen when $A\beta_{40}$ was in the fibrillar conformation, simulations in which the tau fragments interacted with an $A\beta_{40}$ monomer (i.e. non-aggregated) were carried out. The number of hydrogen bonds formed between the Tau4RD or Tau3RD fragments and the $A\beta_{40}$ monomer (Fig. 8a) is considerably lower than it was for the $A\beta_{40}$

template (Fig. 2a). This indicates that Tau4RD and Tau3RD have little affinity for non-aggregated $A\beta_{40}$. Similar simulations carried out with $A\beta_{42}$ show that TauRD's affinity for $A\beta_{42}$ monomers is also low (Fig. S5). Taken together, our results indicate that neither $A\beta_{40}$ or $A\beta_{42}$ monomers can form aggregates in complex with tau. Most likely, when the mix contains $A\beta_{42}$, tau binds to the $A\beta_{42}$ that has already started to form aggregates.

When $A\beta_{40}$ and Tau4RD, or Tau3RD, do form dimers, it is mostly through intermolecular β-sheets involving residues along the C-terminal portion of $A\beta_{40}$ (Fig. 8a). The reason for Tau4RD and Tau3RD associating with the C-terminal half of $A\beta_{40}$, instead of the N-terminal half [as was the case with the $A\beta_{40}$ template (Fig. 2a)], can be found in the secondary structure of the $A\beta_{40}$ monomers. The $_{16}$KLVFFA$_{21}$ region of $A\beta_{40}$, which in the fibril is part of the N-terminal β-strand, and that so efficiently attracts Tau4RD and Tau3RD (Fig. 2a), is more often found in an α-helical conformation in the monomeric state (Fig. 8b). Due to this change in secondary structure, the tau fragments bind to the C-terminal strand instead, which is found in a β-sheet conformation most of the time (see example in Fig. 8c), but to which they seem to have lower affinity. Hence, $A\beta_{40}$ or $A\beta_{42}$ monomers are rarely found in complex with Tau3RD or Tau4RD. As an illustrative example, we built the FEL along the principal components for one of the MD trajectories to describe, in detail, the pathway along which the TauRD and $A\beta_{40}$ monomers form heterodimers (Fig. 9). It should be noted that for this trajectory, after certain time, the $_{16}$KLVFFA$_{21}$ fragment loses the helical secondary structure (representative structure of minimum 6) and adopts the β-stand conformation (representative structure of minimum 7), however the dimer does not change the conformation (Fig. 9).

Conclusions

To summarize, MD trajectories generated with the UNRES force field were used to study the effect of $A\beta_{40}$ fibrils on the aggregation of Tau4RD and Tau3RD, two fragments from the repeat domain of the tau protein. Our results indicate that both Tau3RD and Tau4RD have higher affinity for the $A\beta_{40}$ template than for themselves. $A\beta_{40}$ fibrils act as sticky surfaces onto which the tau fragments easily bind forming intermolecular β-sheets. More importantly, the affinity between Aβ and the tau fragments was not observed when $A\beta_{40}$ or $A\beta_{42}$ were in a non-aggregated form. Put together, these findings might explain why soluble $A\beta_{42}$, but not $A\beta_{40}$, can trigger tau aggregation[11, 14]. The difference might simply be caused by the fact that $A\beta_{42}$ aggregates at a much faster rate than $A\beta_{40}$, and the experiments are comparing the binding of tau to β-rich aggregates of $A\beta_{42}$ with its binding to monomeric $A\beta_{40}$. The results also suggest that other $A\beta_{40}$ fibril polymorphs may sequester Tau3RD and Tau4RD, as long as the $_{16}$KLVFFA$_{21}$ fragment of $A\beta_{40}$ adopts an extended conformation.

Certain limitations of our model deserve some attention. For example, inspection of the different trajectories shows that two chains of Tau4RD or Tau 3RD can form hydrogen bonds with the $A\beta_{40}$ template simultaneously, one on each side of it, and still interact with each other. This is something that could not happen on real fibrils, with typical lengths of at least tens of nm[46]. However, this could happen with pre-fibrillar aggregates that exhibit spherical or disk-shaped morphology[47-48]. NMR and deuterium exchange data indicate that these aggregates have abundant β-sheet conformation, with the C-terminal region buried in

the interior of the structure, and the N-terminal region more exposed to solvent[47-48]. Therefore, the propensity of tau fragments to bind to the N-terminal region of Aβ, when this region is in an extended conformation, indicates that the tau fragments could have high affinity for Aβ's pre-fibrillar aggregates, and thus the aggregates might also be able to trap monomeric tau, preventing it from performing its function, and stabilizing its β-sheet content. Moreover, due to the spherical morphology of the aggregates, and because they are formed by as little as 10 Aβ chains[46-47], several tau fragments could bind to each Aβ aggregate and interact with each other, which might eventually facilitate oligomerization.

Our MD simulations also indicate that the tau fragments have affinity for extended conformations, and thus they might be prone to interacting with other amyloids. Indeed, oligomeric α-synuclein, another protein known to form amyloid fibrils, can also induce tau aggregation[13]. This suggests that Aβ and α-synuclein might not be the only amyloidogenic proteins capable of facilitating tau aggregation

Supplementary Material

Refer to Web version on PubMed Central for supplementary material.

Acknowledgments

This work was supported by grants from the National Institutes of Health (GM-14312) and the National Science Foundation (MCB10-19767). This research was conducted by using the resources of: (a) our 588- processor Beowulf cluster at the Baker Laboratory of Chemistry and Chemical Biology, Cornell University, (b) the supercomputer resources at the Interdisciplinary Center of Mathematical and Computer Modeling (ICM) and (c) the Informatics Center of the Metropolitan Academic Network (IC MAN) in Gdańsk.

References

1. Alzheimer A; Stelzmann RA; Schnitzlein HN; Murtagh FR An English translation of Alzheimer's 1907 paper, "Uber eine eigenartige Erkankung der Hirnrinde". Clin. Anat. 1995, 8, 429–431. [PubMed: 8713166]
2. Selkoe DJ The molecular pathology of Alzheimer's disease. Neuron 1991, 6, 487–498. [PubMed: 1673054]
3. Busciglio J; Lorenzo A; Yeh J; Yankner BA β-Amyloid fibrils induce tau phosphorylation and loss of microtubule binding. Neuron 1995, 14, 879–888. [PubMed: 7718249]
4. Gotz J; Chen F; van Dorpe J; Nitsch RM Formation of neurofibrillary tangles in P301l tau transgenic mice induced by $A\beta_{42}$ fibrils. Science 2001, 293, 1491–1495. [PubMed: 11520988]
5. LaFerla FM Pathways linking Aβ and tau pathologies. Biochem. Soc. Trans. 2010, 38, 993–995. [PubMed: 20658991]
6. Flores-Rodriguez P; Ontiveros-Torres MA; Cardenas-Aguayo MC; Luna-Arias JP; Meraz-Rios MA; Viramontes-Pintos A; Harrington CR; Wischik CM; Mena R; Floran-Garduno B; et al. The relationship between truncation and phosphorylation at the C-terminus of tau protein in the paired helical filaments of Alzheimer's disease. Front. Neurosci. 2015, 9, 33. [PubMed: 25717290]
7. Weingarten MD; Lockwood AH; Hwo SY; Kirschner MW A protein factor essential for microtubule assembly. Proc. Natl. Acad. Sci. U. S. A. 1975, 72, 1858–1862. [PubMed: 1057175]
8. Barghorn S; Mandelkow E Toward a unified scheme for the aggregation of tau into Alzheimer paired helical filaments. Biochemistry 2002, 41, 14885–14896. [PubMed: 12475237]
9. Hardy J; Selkoe DJ The amyloid hypothesis of Alzheimer's disease: progress and problems on the road to therapeutics. Science 2002, 297, 353–356. [PubMed: 12130773]
10. Masters CL; Selkoe DJ Biochemistry of amyloid β-protein and amyloid deposits in Alzheimer disease. Cold Spring Harb. Perspect. Med. 2012, 2, a006262. [PubMed: 22675658]

11. Rank KB; Pauley AM; Bhattacharya K; Wang Z; Evans DB; Fleck TJ; Johnston JA; Sharma SK Direct interaction of soluble human recombinant tau protein with Aβ 1–42 results in tau aggregation and hyperphosphorylation by tau protein kinase II. FEBS Lett. 2002, 514, 263–268. [PubMed: 11943163]
12. Guo JP; Arai T; Miklossy J; McGeer PL Aβ and tau form soluble complexes that may promote self aggregation of both into the insoluble forms observed in Alzheimer's disease. Proc. Natl. Acad. Sci. U. S. A. 2006, 103, 1953–1958. [PubMed: 16446437]
13. Lasagna-Reeves CA; Castillo-Carranza DL; Guerrero-Muoz MJ; Jackson GR; Kayed R Preparation and characterization of neurotoxic tau oligomers. Biochemistry 2010, 49, 10039–10041. [PubMed: 21047142]
14. Hu X; Li X; Zhao M; Gottesdiener A; Luo W; Paul S Tau pathogenesis is promoted by Aβ1–42 but not Aβ1–40. Mol. Neurodegener. 2014, 9, 52. [PubMed: 25417177]
15. Stine WB Jr.; Dahlgren KN; Krafft GA; LaDu MJ In vitro characterization of conditions for amyloid-β peptide oligomerization and fibrillogenesis. J. Biol. Chem. 2003, 278, 11612–11622. [PubMed: 12499373]
16. Tycko R Amyloid polymorphism: structural basis and neurobiological relevance. Neuron 2015, 86, 632–645. [PubMed: 25950632]
17. Liwo A; Czaplewski C; Pillardy J; Scheraga HA Cumulant-based expressions for the multibody terms for the correlation between local and electrostatic interactions in the united-residue force field. J. Chem. Phys. 2001, 115, 2323–2347.
18. Ołdziej S; Łągiewka J; Liwo A; Czaplewski C; Chinchio M; Nanias M; Scheraga HA Optimization of the UNRES Force Field by Hierarchical Design of the Potential-Energy Landscape. 3. Use of Many Proteins in Optimization. J. Phys. Chem. B 2004, 108, 16950–16959.
19. Liwo A; Khalili M; Czaplewski C; Kalinowski S; Ołdziej S; Wachucik K; Scheraga HA Modification and optimization of the united-residue (UNRES) potential energy function for canonical simulations. I. Temperature dependence of the effective energy function and tests of the optimization method with single training proteins. J. Phys. Chem. B 2007, 111, 260–285. [PubMed: 17201450]
20. Liwo A; Czaplewski C; Ołdziej S; Rojas AV; Kazmierkiewicz R; Makowski M; Murarka RK; Scheraga HA Simulation of Protein Structure and Dynamics with the Coarse-Grained UNRES Force Field In Coarse-Graining of Condensed Phase and Biomolecular Systems, Voth G, Ed. CRC Press: 2008; pp 107–122.
21. Maisuradze GG; Senet P; Czaplewski C; Liwo A; Scheraga HA Investigation of protein folding by coarse-grained molecular dynamics with the UNRES force field. J. Phys. Chem. A 2010, 114, 4471–4485. [PubMed: 20166738]
22. Rojas AV; Liwo A; Scheraga HA Molecular dynamics with the United-residue force field: ab initio folding simulations of multichain proteins. J. Phys. Chem. B 2007, 111, 293–309. [PubMed: 17201452]
23. He Y; Xiao Y; Liwo A; Scheraga HA Exploring the parameter space of the coarse-grained UNRES force field by random search: selecting a transferable medium-resolution force field. J. Comput. Chem. 2009, 30, 2127–2135. [PubMed: 19242966]
24. Petkova AT; Yau WM; Tycko R Experimental constraints on quaternary structure in Alzheimer's β-amyloid fibrils. Biochemistry 2006, 45, 498–512. [PubMed: 16401079]
25. Rojas A; Liwo A; Browne D; Scheraga HA Mechanism of fiber assembly: treatment of Aβ peptide aggregation with a coarse-grained united-residue force field. J. Mol. Biol. 2010, 404, 537–552. [PubMed: 20888834]
26. Khalili M; Liwo A; Jagielska A; Scheraga HA Molecular dynamics with the united-residue model of polypeptide chains. II. Langevin and Berendsen-bath dynamics and tests on model α-helical systems. J. Phys. Chem. B 2005, 109, 13798–13810. [PubMed: 16852728]
27. Khalili M; Liwo A; Rakowski F; Grochowski P; Scheraga HA Molecular dynamics with the united-residue model of polypeptide chains. I. Lagrange equations of motion and tests of numerical stability in the microcanonical mode. J. Phys. Chem. B 2005, 109, 13785–13797. [PubMed: 16852727]

28. Berendsen HJC; Postma JPM; Gunsteren WFV; DiNola A; Haak JR Molecular dynamics with coupling to an external bath. J. Chem. Phys. 1984, 81, 3684–3690.
29. Goedert M; Spillantini MG; Jakes R; Rutherford D; Crowther RA Multiple isoforms of human microtubule-associated protein tau: sequences and localization in neurofibrillary tangles of Alzheimer's disease. Neuron 1989, 3, 519–526. [PubMed: 2484340]
30. Goedert M; Jakes R Expression of separate isoforms of human tau protein: correlation with the tau pattern in brain and effects on tubulin polymerization. EMBO J. 1990, 9, 4225–4230. [PubMed: 2124967]
31. Goedert M; Spillantini MG A century of Alzheimer's disease. Science 2006, 314, 777–781. [PubMed: 17082447]
32. Wegmann S; Medalsy ID; Mandelkow E; Müller DJ The fuzzy coat of pathological human Tau fibrils is a two-layered polyelectrolyte brush. Proc. Natl. Acad. Sci. U. S.A. 2013, 110, E313–E321. [PubMed: 23269837]
33. von Bergen M; Friedhoff P; Biernat J; Heberle J; Mandelkow EM; Mandelkow E Assembly of τ protein into Alzheimer paired helical filaments depends on a local sequence motif ((306)VQIVYK(311)) forming β structure. Proc. Natl. Acad. Sci. U. S. A. 2000, 97, 5129–5134. [PubMed: 10805776]
34. Goux WJ; Kopplin L; Nguyen AD; Leak K; Rutkofsky M; Shanmuganandam VD; Sharma D; Inouye H; Kirschner DA The formation of straight and twisted filaments from short tau peptides. J. Biol. Chem. 2004, 279, 26868–26875. [PubMed: 15100221]
35. Li W; Lee VM Characterization of two VQIXXK motifs for tau fibrillization in vitro. Biochemistry 2006, 45, 15692–15701. [PubMed: 17176091]
36. Wiltzius JJ; Landau M; Nelson R; Sawaya MR; Apostol MI; Goldschmidt L; Soriaga AB; Cascio D; Rajashankar K; Eisenberg D Molecular mechanisms for protein-encoded inheritance. Nat. Struct. Mol. Biol. 2009, 16, 973–978. [PubMed: 19684598]
37. Maisuradze GG; Liwo A; Scheraga HA Principal component analysis for protein folding dynamics. J. Mol. Biol. 2009, 385, 312–329. [PubMed: 18952103]
38. Maisuradze GG; Liwo A; Scheraga HA How adequate are one- and two-dimensional free energy landscapes for protein folding dynamics? Phys. Rev. Lett. 2009, 102, 238102. [PubMed: 19658975]
39. Maisuradze GG; Liwo A; Scheraga HA Relation between free energy landscapes of proteins and dynamics. J. Chem. Theory Comput. 2010, 6, 583–595. [PubMed: 23620713]
40. Tjernberg LO; Callaway DJ; Tjernberg A; Hahne S; Lilliehook C; Terenius L; Thyberg J; Nordstedt C A molecular model of Alzheimer amyloid β-peptide fibril formation. J. Biol. Chem. 1999, 274, 12619–12625. [PubMed: 10212241]
41. Rojas A; Maisuradze N; Kachlishvili K; Scheraga HA; Maisuradze GG Elucidating Important Sites and the Mechanism for Amyloid Fibril Formation by Coarse-Grained Molecular Dynamics. ACS Chem. Neurosci. 2017, 8, 201–209. [PubMed: 28095675]
42. Landau M; Sawaya MR; Faull KF; Laganowsky A; Jiang L; Sievers SA; Liu J; Barrio JR; Eisenberg D Towards a pharmacophore for amyloid. PLoS Biol. 2011, 9, e1001080. [PubMed: 21695112]
43. Qi R; Luo Y; Wei G; Nussinov R; Ma B Aβ “stretching-and-packing” cross-seeding mechanism can trigger tau protein aggregation. J. Phys. Chem. Lett 2015, 6, 3276–3282.
44. Mylonas E; Hascher A; Bernado P; Blackledge M; Mandelkow E; Svergun DI Domain conformation of tau protein studied by solution small-angle X-ray scattering. Biochemistry 2008, 47, 10345–10353. [PubMed: 18771286]
45. McGowan E; Pickford F; Kim J; Onstead L; Eriksen J; Yu C; Skipper L; Murphy MP; Beard J; Das P; et al. $A\beta_{42}$ is essential for parenchymal and vascular amyloid deposition in mice. Neuron 2005, 47, 191–199. [PubMed: 16039562]
46. Dubnovitsky A; Sandberg A; Rahman MM; Benilova I; Lendel C; Hard T Amyloid-β protofibrils: size, morphology and synaptotoxicity of an engineered mimic. PLoS One 2013, 8, e66101. [PubMed: 23843949]

47. Chimon S; Shaibat MA; Jones CR; Calero DC; Aizezi B; Ishii Y Evidence of fibril-like β-sheet structures in a neurotoxic amyloid intermediate of Alzheimer's β-amyloid. Nat. Struct. Mol. Biol. 2007, 14, 1157–1164. [PubMed: 18059284]

48. Ahmed M; Davis J; Aucoin D; Sato T; Ahuja S; Aimoto S; Elliott JI; Van Nostrand WE; Smith SO Structural conversion of neurotoxic amyloid-β_{1-42} oligomers to fibrils. Nat. Struct. Mol. Biol. 2010, 17, 561–567. [PubMed: 20383142]

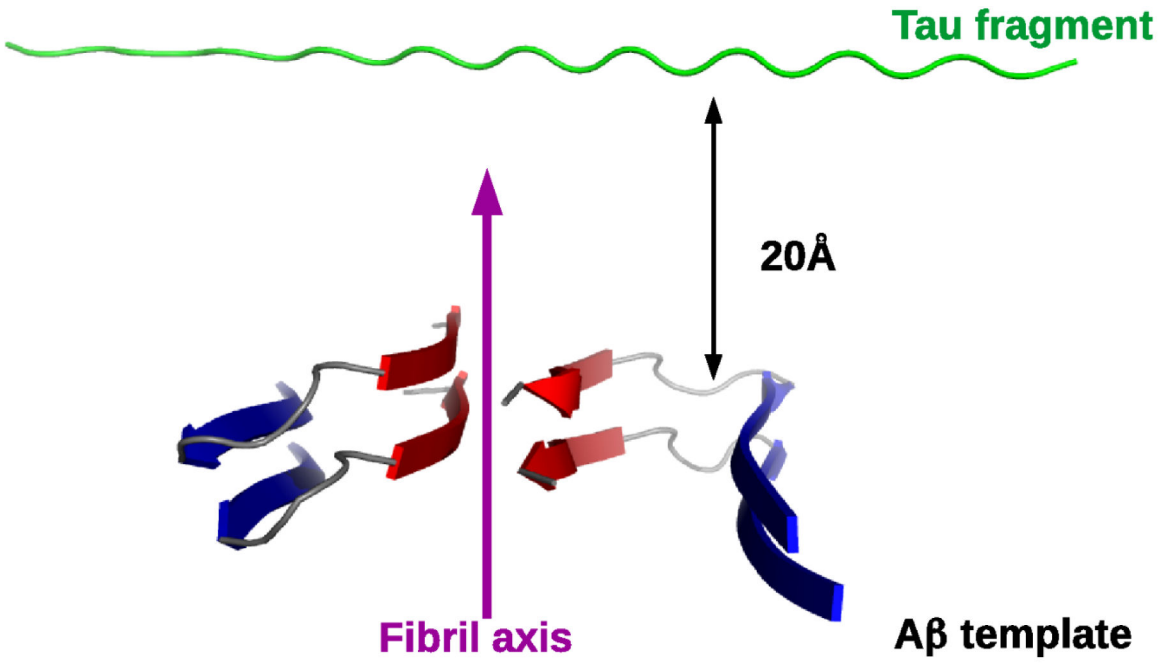

Figure 1:
Simulation Setup. A two-layers (4 chains) fibril, based on the model of Petkova et al[24] for $A\beta_{40}$ fibrils, was used as a template to simulate the interaction between an $A\beta_{40}$ fibril and the repeat fragment from tau protein. The N-terminal and C-terminal strands of the $A\beta_{40}$ are colored in blue and red, respectively. Distance restraints were used to stabilize the template, but no restraints were applied on the monomer. The monomer was initially placed at a 20 Å distance from the template in a completely unfolded conformation. The tau fragment (green color) was either Tau3RD, Tau4RD, R1, R2, R3 or R4.

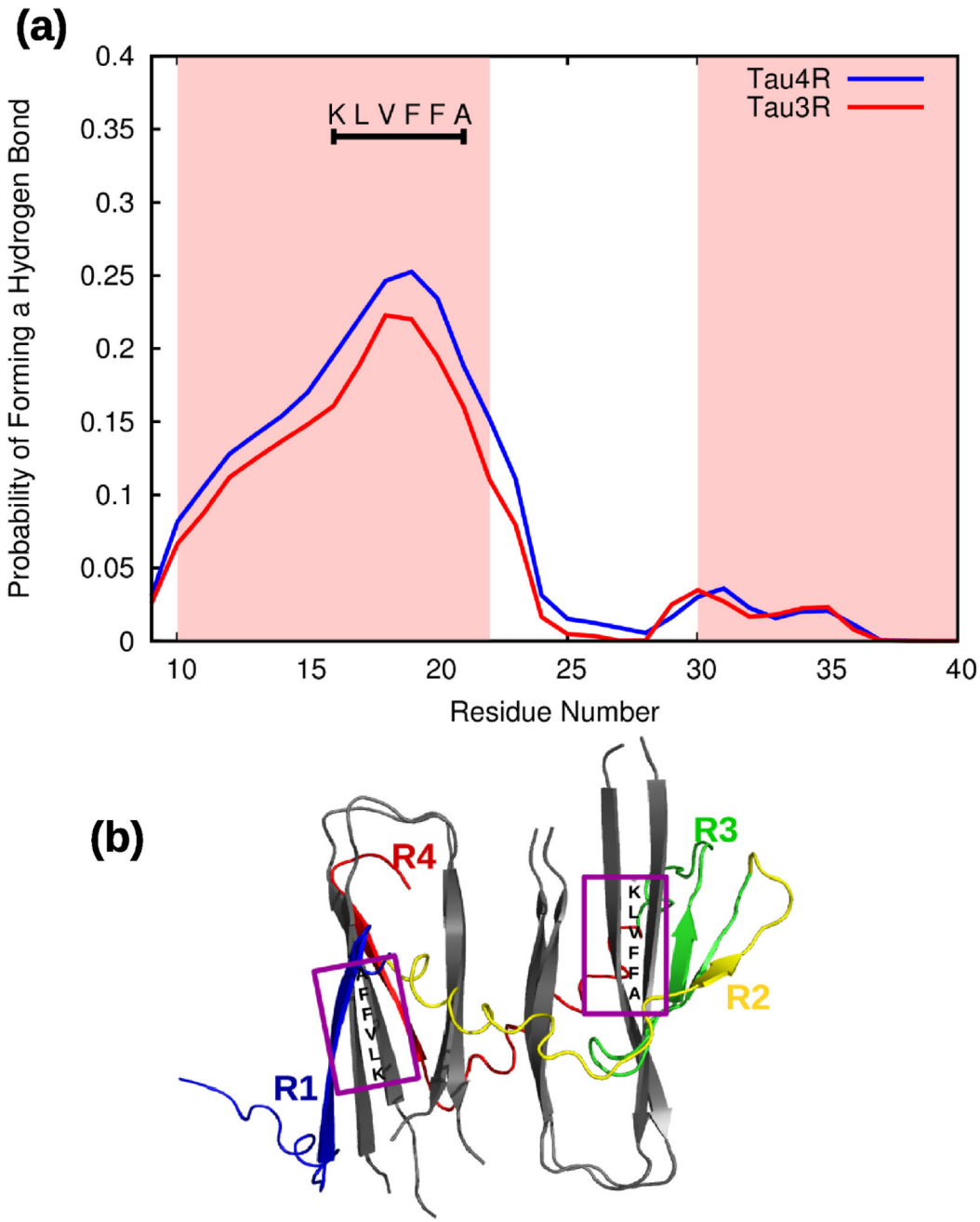

Figure 2.

Simulations of Tau3RD or Tau4RD and an Aβ_{40} fibril template. (a) The probability for each residue in the Aβ peptides of forming a hydrogen bond with any of the residues in the Tau monomer. The two regions along the Aβ peptides that adopt a β-sheet conformation are shaded in pink. Hydrogen bonding occurs mainly along the N-terminal strand of the Aβ peptides. The region with the highest probability, residues 16-21, is indicated by a horizontal black line, as well as the sequence along this fragment. (b) Representative snapshot showing the binding of Tau4RD and the Aβ_{40} template (gray). Different colors are used for each of

the tau repeats: R1 in blue, R2 in yellow, R3 in green and R4 in red. A purple box indicates the KLVFFA fragment on $A\beta_{40}$.

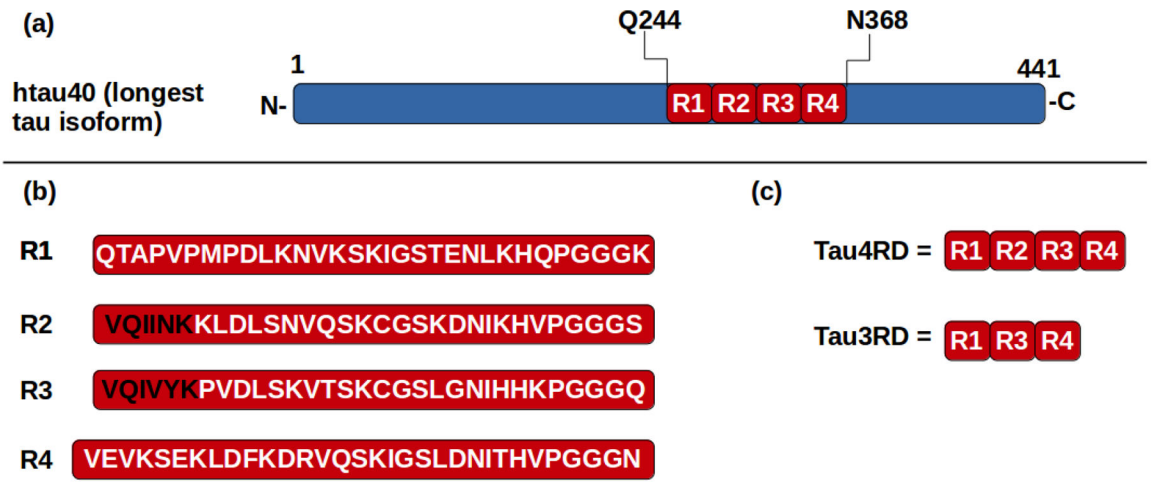

Figure 3.

(a) Representation of the longest tau isoform, htau40, showing the location of the repeat domain (R1 to R4). (b) The sequence of each of the four repeats, R1, R2, R3 and R4. The two fragments known to form fibrils by themselves[34, 36] and to be crucial for tau fibrillization[35] are shown in black. (c) Composition of Tau3RD and Tau4RD fragments.

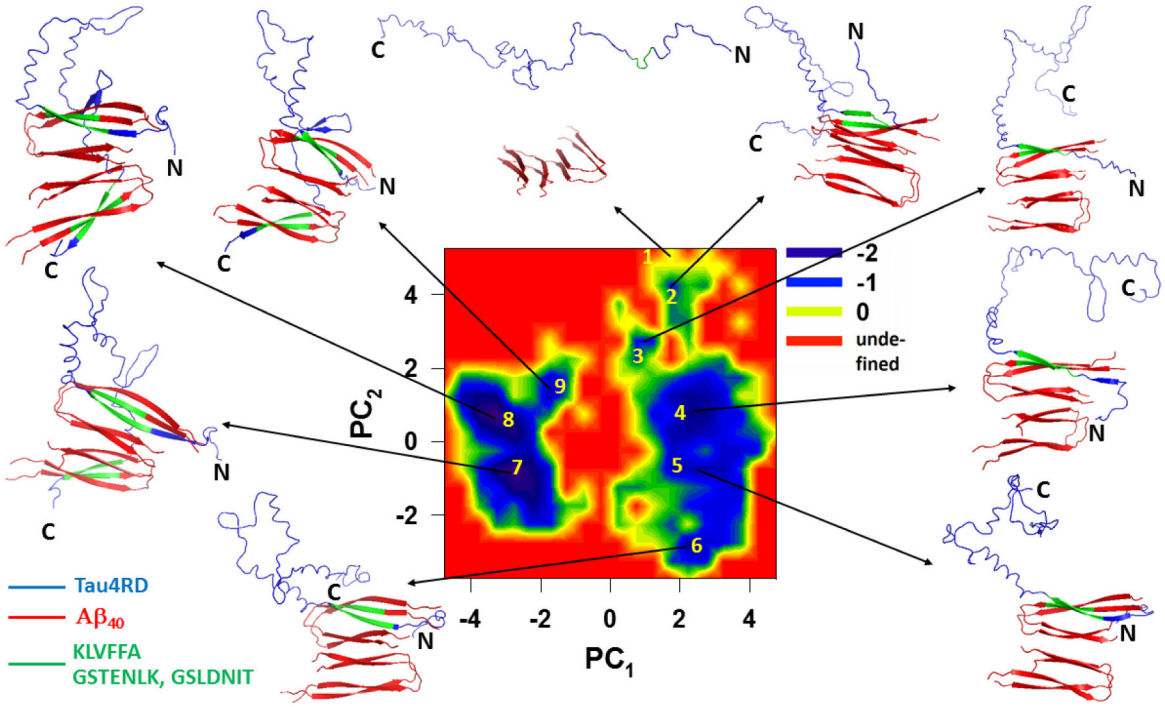

Figure 4.

Free-energy landscape (in kcal/mol) along the first two PCs, μ (PC1, PC2) = - k_BT ln P (PC_1, PC_2), with representative structures at the minima (labeled 1 to 9) for the trajectory of tau protein binding to the $A\beta_{40}$ template.

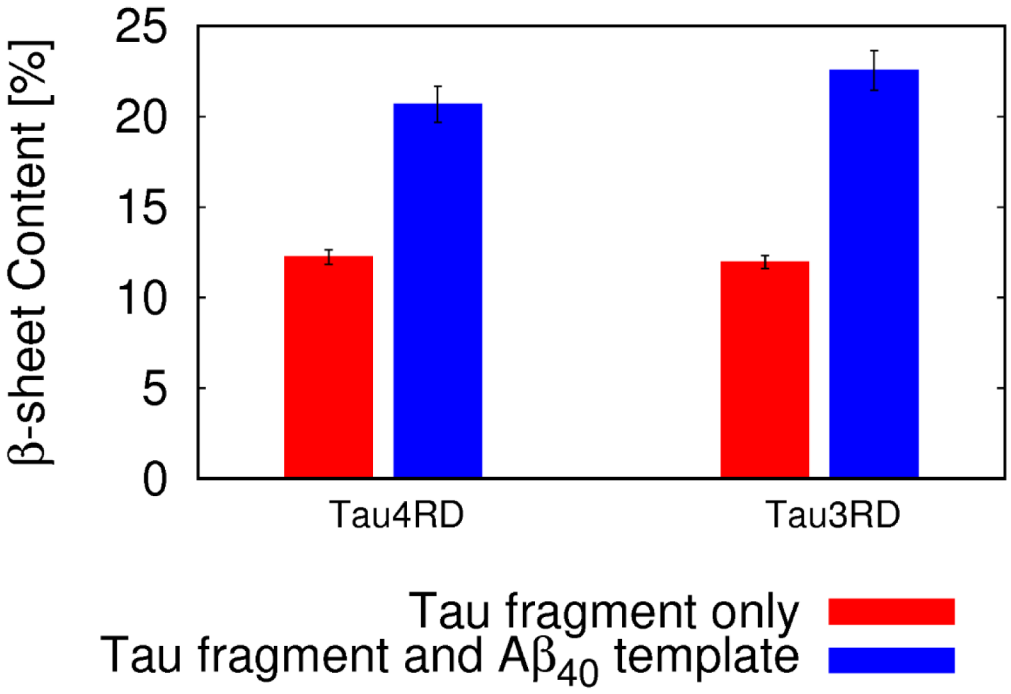

Figure 5:

The β-sheet content (in %) of Tau3RD and Tau4RD fragments in the absence (red) or presence (blue) of the $A\beta_{40}$ template. The errors were obtained from fluctuations between the different trajectories.

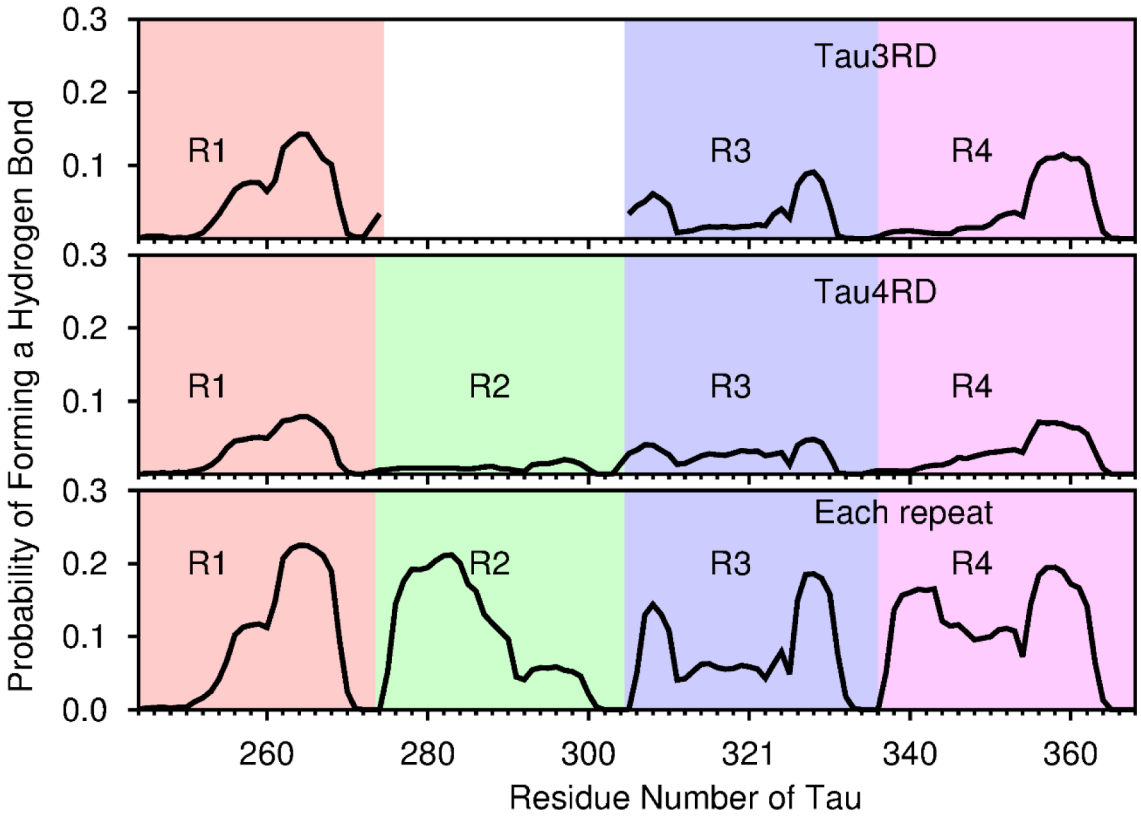

Figure 6.

The probability for each residue in Tau3RD (top), Tau4RD (middle), or any of the repeats independently (bottom), of forming a hydrogen bond with any of the residues from the Aβ chains. The results from simulations of each of the repeats independently are shown next to each other to facilitate comparison with the upper panels. The regions corresponding to each of the repeats is indicated by different background colors, pink (R1), green (R2), blue (R3) and purple (R4). Numbering of residues corresponds to the longest Tau isoform, with R1=244-274, R2=275-305, R3=306-336 and R3=337-368. For top plot (Tau3RD), the region corresponding to the second repeat is empty because this region does not exist in Tau3RD.

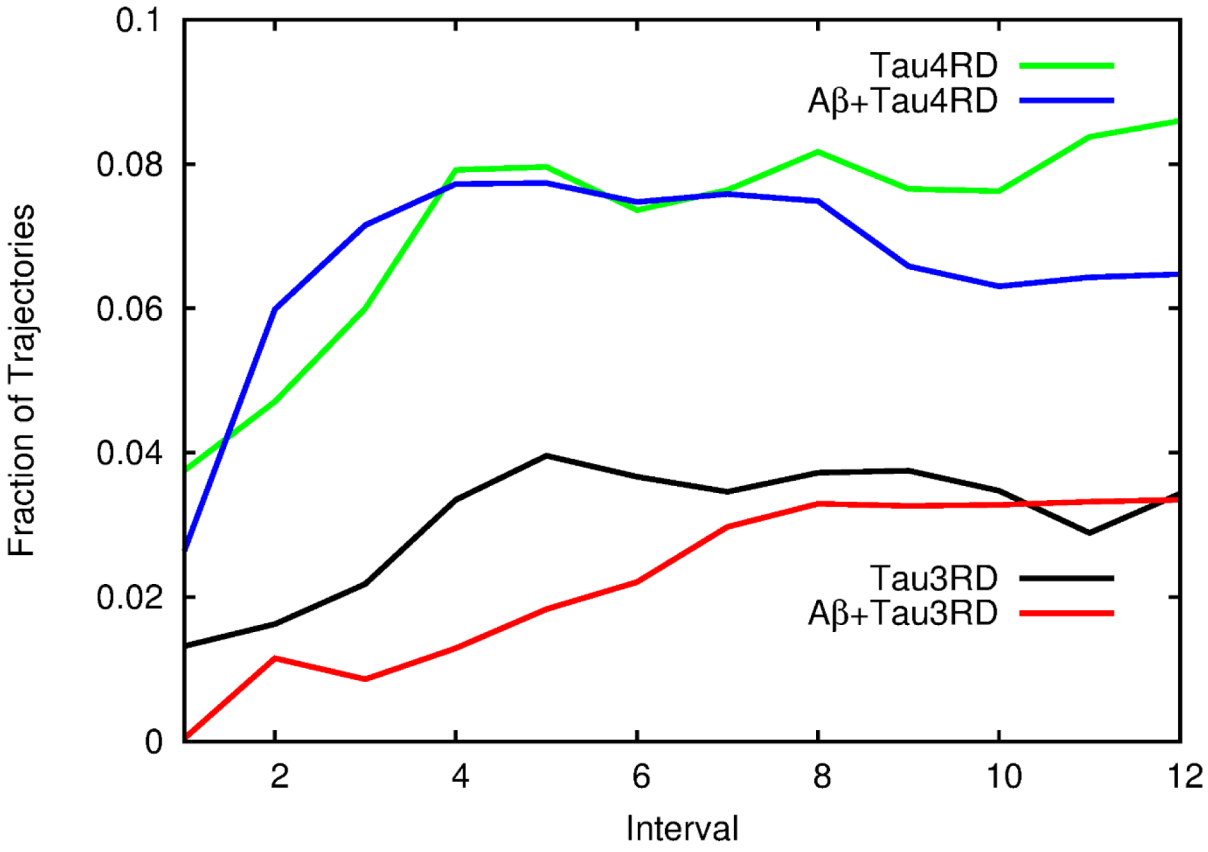

Figure 7:

The effect of the $A\beta_{40}$ template on dimer formation by Tau3RD or Tau4RD. The trajectories were divided into 12 equal intervals, and the fraction of trajectories in which an intermolecular β-sheet was formed between the two tau monomers (either Tau3RD or Tau4RD) is shown at each interval. Values are shown for Tau4RD in the absence (yellow) or presence (blue) of the template and for Tau3RD in the absence (black) or presence (red) of the template.

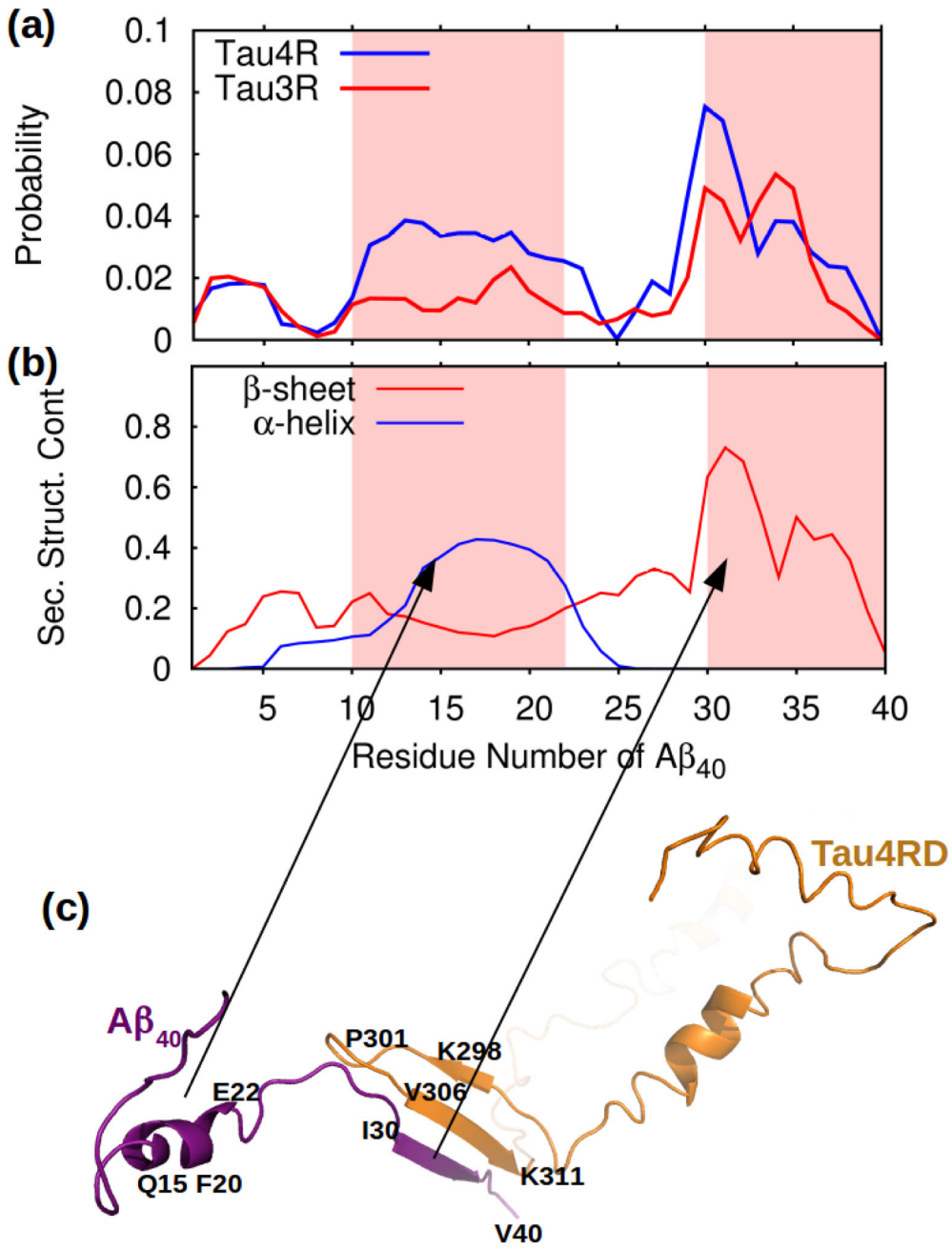

Figure 8.

Simulations of dimerization between $A\beta_{40}$ and TauRD (a) The probability that each of the residues along the $A\beta_{40}$ sequence would have formed a hydrogen bond with any of the residues in Tau4RD (blue) or Tau3RD (red). The regions that in the fibrils are in a β-strand conformation are shaded in pink. (b) β-sheet and α-helix content for along the $A\beta_{40}$ sequence. (c) Example of a dimer formed between Tau4RD (orange) and $A\beta_{40}$ (purple) illustrating the higher tendency to form hydrogen bonds along the C-terminal region of $A\beta_{40}$.

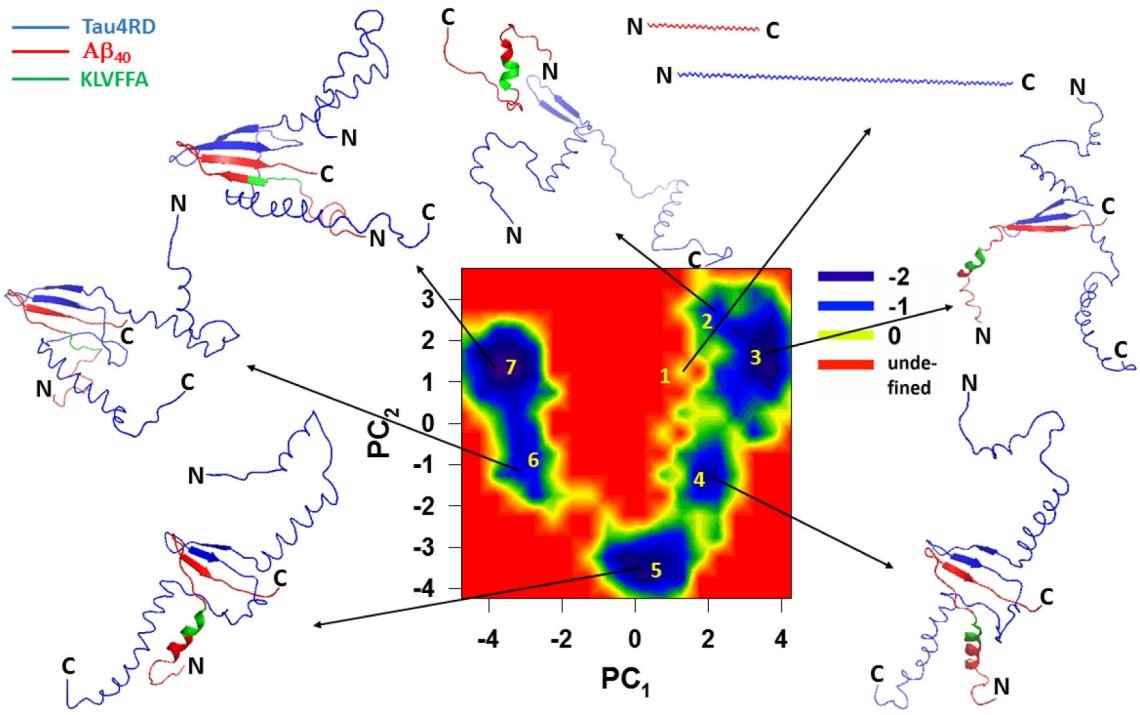

Figure 9.

Free-energy landscape (in kcal/mol) along the first two PCs with representative structures at the minima (labeled 1 to 7) for the trajectory of tau protein binding to the $A\beta_{40}$ monomer.